Intramolecular End-to-End Excimer Formation of Bis((1-pyrenylmethoxy)carbonyl)alkanes. A Study of End-to-End Collisional Frequency on a Chain Molecule

T. Kanaya, K. Goshiki, M. Yamamoto,* and Y. Nishijima*

Contribution from the Department of Polymer Chemistry, Kyoto University, Kyoto 606, Japan.
Received January 27, 1981

Abstract: Intramolecular end-to-end excimer formation of a series of bis((1-pyrenylmethoxy)carbonyl)alkanes (n = 1-22) in 2-methyltetrahydrofuran has been studied under photostationary and transient states in the temperature range from -130 to 25 °C. The results were analyzed in terms of Förster's reaction kinetics to obtain the rate constant for the intramolecular excimer formation k_a, which corresponds to the intramolecular end-to-end collisional frequency. It was found that k_a is approximately proportional to the -1.5 power of the chain length in the temperature region above -60 °C. On the basis of these results, dynamic behavior of the samples was discussed. The temperature dependence of k_a for each sample gave an apparent activation energy of ca. 5 kcal/mol. The activation energy was analyzed by two treatments to evaluate the energy-barrier height for the internal rotation of the chain. The strain of a chain, which was produced in forming the intramolecular end-to-end excimer, was also discussed on the basis of the characteristic properties of excimer emission.

Many investigations have been carried out on intramolecular end-to-end reactions on a polymer chain in solution. The reactions are conveniently classified into "chemical reactions" and "diffusion-controlled reactions". "Chemical reactions" are also qualified by "chemical processes with appreciable activation energies",[1] which are called "activation-controlled reactions". Studies on intramolecular chemical reactions[2-9] provide equilibrium properties of a polymer chain, since the rate of the chemical reaction on a polymer chain is determined by the ring-closure probability of the polymer chain in equilibrium. Recently, some studies of intramolecular end-to-end diffusion-controlled reactions[10-21] have appeared. In contrast to the intramolecular chemical reactions, the rate of the diffusion-controlled reactions on a polymer chain is determined by the frequency of collisions between both end groups. Therefore, study of these phenomena gives information on the rate of conformational transition or on the dynamic behavior of a polymer chain. Only a few methods deal with end-to-end collisional frequency on a polymer chain, though a number of techniques are used for the investigation of local or collective motion of polymer chains, e.g., NMR relaxation,[22] ESR spin probe,[23] fluorescence depolarization,[24] excimer emission,[25] ultrasonic absorption,[26] dynamic light scattering,[27] inelastic and quasi-elastic neutron scattering,[28] dielectric relax-

(1) The classification of the reactions into "chemical reactions" and "diffusion-controlled reactions" is very convenient but ambiguous. Strictly speaking, the reactions should be classified by a mutual relation between intrinsic relaxation time of the reaction k^{-1} and that of molecular motion of a chain ρ. Here, k is the intrinsic rate of the reaction. According to the language of k and ρ, "chemical reactions" are qualified by the relation of $k^{-1} \gg \rho$. Most of these chemical reactions have appreciable activation energies. "Diffusion-controlled reactions" are qualified by $k^{-1} \ll \rho$.

(2) Stoll, M.; Rouvé, A. *Helv. Chim. Acta* **1935**, *18*, 1087.

(3) Semlyen, J. *Adv. Polym. Sci.* **1976**, *21*, 42.

(4) Morawetz, H. "Macromolecules in Solutions", 2nd ed.; Wiley-Interscience: New York, 1975; Chapter IX-C.

(5) (a) Winnik, M. A.; Trueman, R. E.; Jackowski, G.; Saunders, D. S.; Whittigton, S. G. *J. Am. Chem. Soc.* **1974**, *96*, 4843. (b) Winnik, M. A.; Basu, S. M.; Lee, C. K.; Saunders, D. S. *Ibid.* **1976**, *98*, 2928. (c) Winnik, M. A. *Acc. Chem. Res.* **1977**, *10*, 173. (d) Saunders, D. S.; Winnik, M. A. *Macromolecules* **1978**, *11*, 18. (e) Saunders, D. S.; Winnik, M. A. *Ibid.* **1978**, *11*, 25.

(6) (a) Sisido, M. *Macromolecules* **1971**, *4*, 737. (b) Sisido, M.; Mitamura, T.; Imanishi, Y.; Higashimura, T. *Ibid.* **1976**, *9*, 320. (c) Sisido, M.; Higashimura, T. *Ibid.* **1976**, *9*, 389. (d) Sisido, M.; Takagi, H.; Imanishi, Y.; Higashimura, T. *Ibid.* **1977**, *10*, 125. (e) Takagi, H.; Sisido, M.; Imanishi, Y.; Higashimura, T. *Bull. Chem. Soc. Jpn.* **1977**, *50*, 1807. (f) Sisido, M.; Yoshikawa, E.; Imanishi, Y.; Higashimura, T. *Ibid.* **1978**, *51*, 1464. (g) Sisido, M.; Imanishi, Y.; Higashimura, T. *Ibid.* **1978**, *51*, 1469.

(7) Breslow, R.; Rothbard, J.; Herman, F.; Rodriguez, M. L. *J. Am. Chem. Soc.* **1978**, *100*, 1213.

(8) (a) Galli, C.; Illuminati, G.; Mandolini, L.; Tamborra, P. *J. Am. Chem. Soc.* **1977**, *99*, 2591. (b) Illuminati, G.; Mandolini, L.; Masci, B. *J. Am. Chem. Soc.* **1977**, *99*, 6308.

(9) (a) Put, J.; De Schryver, F. C. *Ibid.* **1973**, *95*, 137. (b) De Schryver, F. C.; Put, J.; Loos, H. *Ibid.* **1974**, *96*, 6994.

(10) (a) Connor, H. D.; Shimada, K.; Szwarc, M. *Chem. Phys. Lett.* **1972**, *14*, 402. (b) Shimada, K.; Szwarc, M. *Ibid.* **1974**, *28*, 540. (c) Szwarc, M.; Shimada, K. *J. Polym. Sci., Polym. Symp.* **1974**, *46*, 193. (d) Shimada, K.; Szwarc, M. *J. Am. Chem. Soc.* **1975**, *97*, 3313. (e) Shimada, K.; Szwarc, M. *Ibid.* **1975**, *97*, 3321. (f) Sisido, M.; Shimada, K. *Ibid.* **1977**, *99*, 7785.

(11) Nairn, J. A.; Braun, C. L.; Caluwe, P.; Szwarc, M. *Chem. Phys. Lett.* **1978**, *54*, 469.

(12) Zachariasse, K.; Kühnle, W. *Z. Phys. Chem. (Wiesbaden)* **1976**, *101*, 267.

(13) Yamamoto, M.; Goshiki, K.; Kanaya, T.; Nishijima, Y. *Chem. Phys. Lett.* **1978**, *56*, 333.

(14) (a) Cuniberti, C.; Perico, A. *Eur. Polym. J.* **1977**, *13*, 369. (b) Perico, A.; Cuniberti, C. *J. Polym. Sci., Polym. Phys. Ed.* **1977**, *15*, 1435. (c) Cuniberti, C.; Perico, A. *Ann. N.Y. Acad. Sci.* **1981**, *366*, 35.

(15) Goldenberg, M.; Emert, J.; Morawetz, H. *J. Am. Chem. Soc.* **1978**, *100*, 7171.

(16) (a) Winnik, M. A.; Redpath, T.; Richards, D. H. *Macromolecules* **1980**, *13*, 328. (b) Redpath, A. E. C.; Winnik, M. A. *Ann. N.Y. Acad. Sci.* **1981**, *366*, 75. (c) Redpath, A. E. C.; Winnik, M. A. *J. Am. Chem. Soc.* **1980**, *102*, 6869.

(17) Halpern, A. H.; Legenza, M. W.; Ramachandran, B. R. *J. Am. Chem. Soc.* **1979**, *101*, 5736.

(18) (a) Yamamoto, M.; Hatano, Y.; Nishijima, Y. *Chem. Lett.* **1976**, 351. (b) Hatano, Y.; Yamamoto, M.; Nishijima, Y. *J. Phys. Chem.* **1978**, *82*, 367.

(19) Haas, E.; Katchalski-Katzir, E.; Steinberg, I. Z. *Biopolymer* **1978**, *17*, 11.

(20) Sisido, M.; Imanishi, Y.; Higashimura, T. *Macromolecules* **1979**, *12*, 975.

(21) (a) Ushiki, H.; Horie, K.; Okamoto, A.; Mita, I. *Polym. J.* **1981**, *13*, 191. (b) Mita, I. *Ann. N.Y. Acad. Sci.* **1981**, *366*, 62.

(22) (a) Schaefer, J. In "Structural Studies of Macromolecules by Spectroscopic Methods"; Ivin, K. J., Ed.; Wiley-Interscience: New York, 1976; Chapter 11. (b) Levy, G. C.; Axelson, D. E.; Schwartz, R.; Hochmann, J. *J. Am. Chem. Soc.* **1978**, *100*, 410. (c) Tsutsumi, A.; Perly, B.; Forchioni, A.; Chachaty, C. *Macromolecules* **1978**, *11*, 977. (d) Lang, M. C.; Laupretre, F.; Nose, C.; Monnerie, L. *J. Chem. Soc., Faraday Trans. 2* **1979**, *75*, 349.

(23) (a) Törmälä, P. *J. Macromol. Sci. Rev. Macromol. Chem.* **1979**, *C17*, 297. (b) Bullock, A. T.; Cameron, G. In "Structural Studies of Macromolecules by Spectroscopic Methods"; Ivin, K. J., Ed.; Wiley-Interscience: New York, 1976; Chapter 15.

(24) Nishijima, Y., In "Progress in Polymer Science. Japan"; Onogi, S., Uno, K., Eds.; Kodansha: Tokyo, Wiley: New York, 1973; Vol. 6, p 199.

(25) Liao, T. P.; Morawetz, H. *Macromolecules* **1980**, *13*, 1228.

(26) (a) Piercy, J. E.; Seshagiri Rao, M. G. *J. Chem. Phys.* **1967**, *46*, 3951. (b) Bell, W.; North, A. M.; Pethrich, R. A.; Poh, B. T. *J. Chem. Soc., Faraday Trans. 2* **1979**, *75*, 1115.

(27) Berne, B. J.; Pecora, R. "Dynamic Light Scattering"; Wiley-Interscience: New York, 1976.

(28) (a) Higgins, J. S.; Allen, G.; Brier, P. N. *Polymer* **1972**, *13*, 159. (b) Allen, G.; Ghosh, R.; Higgins, J. S.; Cotton, J. P.; Farnoux, B.; Jannik, G.; Weill, G. *Chem. Phys. Lett.* **1976**, *38*, 577. (c) Higgins, J. S.; Allen, G.; Ghosh, R. E.; Howells, W. S.; Farnoux, B. *Ibid.* **1977**, *49*, 197. (d) Allen, G. *Makromol. Chem. Suppl.* **1979**, *3*, 335. (e) Ewen, B.; Stobl, G. R.; Richter, D. *Faraday Discuss. Chem. Soc.* **1980**, *69*, 19. (f) Nicholson, L. K.; Higgins, J. S.; Hayter, J. B. In "Neutron Spin Echo"; Mezei, F., Ed.; Springer-Verlag: Berlin, Heidelberg, 1980; Chapter 2, p 75.

0002-7863/82/1504-3580$01.25/0

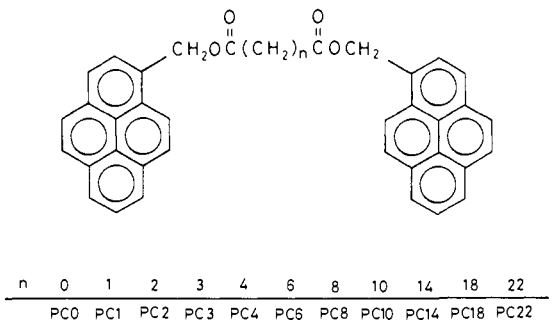

Figure 1.

ation,[29] and rheological relaxation.[30] From this point of view, any investigation of an intramolecular end-to-end diffusion-controlled reaction is an important method for studying chain dynamics.

Various diffusion-controlled reactions have been employed for such studies. Shimada et al.[10] determined the frequency of end-to-end collisions by the analysis of ESR line shapes for intramolecular end-to-end electron transfers in α-N-$(CH_2)_n$-α-N$^{-}\cdot$ (α-N = α-naphthyl group) and PI-$(CH_2)_n$-PI$^{-}\cdot$ (PI = phthalimidoyl group) systems. Fluorescence phenomena, such as fluorescence quenching,[11] excimer formation,[12-17] exciplex formation,[18] and energy transfer,[19,20] have been used for the study of chain dynamics. Recently, triplet probes have been used by Ushiki et al.[21] They studied the delayed fluorescence of anthryl groups attached at a polystyrene chain end and obtained the intramolecular end-to-end collisional frequency between two end groups.

In previous preliminary work,[13] we have reported intramolecular end-to-end excimer emission behavior of a series of bis((1-pyrenylmethoxy)carbonyl)alkanes under photostationary conditions. In the present work, time-resolved measurements in addition to the photostationary measurements were carried out, and the intramolecular end-to-end excimer formation was investigated in relation to the dynamics of flexible chains. Structures of a series of bis((1-pyrenylmethoxy)carbonyl)alkanes (PC0, PC1, ..., PC22) are shown in Figure 1. All of the measurements were taken at temperatures from −130 to 25 °C in 2-methyltetrahydrofuran (MTHF) solution. The lifetime of the excited pyrene group is 250 ns in MTHF, so that it is an appropriate probe for investigation of the relaxation phenomena in the time range 10^{-9}–10^{-7} s. We have analyzed the experimental data in terms of Förster's reaction kinetics and determined the rate constant of intramolecular end-to-end excimer formation as a function of the chain length and of the temperature. 1-Pyrenylmethyl butanoate (MC4) was used as a model compound to compare the intramolecular excimer with the intermolecular one.

Experimental Section

Preparation of Materials. A series of bis((1-pyrenylmethoxy)carbonyl)alkanes was synthesized by the esterification of the corresponding alkanedicarboxylic acid chloride with 1-pyrenylmethylol that had been prepared by the reduction of 1-pyrenylmethylol with sodium borohydride in the usual manner. Each alkanedicarboxylic acid chloride was prepared by the reaction of the corresponding alkanedicarboxylic acid with thionyl chloride. The corresponding alkanedicarboxylic acid chloride dissolved in chloroform was then gradually added to the solution of 1-pyrenylmethylol and triethylamine in chloroform. The reaction mixture was refluxed for 2 h, and the solvent was evaporated after washing with water. The product was recrystallized several times from ethanol and tetrahydrofuran (5:1), further purified by column chromatography on silica gel with benzene, and finally recrystallized from ethanol.

Structures of these compounds were confirmed by 100-MHz NMR spectroscopy and elemental analysis. The melting points of bis((1-pyrenylmethoxy)carbonyl)alkanes were as follows: PC1, 171–173 °C; PC2, 193–194 °C; PC3, 148–151 °C; PC4, 143–145 °C; PC6, 126–128 °C; PC8, 127–128 °C; PC10, 106–108 °C; PC14, 108–109 °C; PC18, 116–118 °C; PC22, 109–111 °C; and PC0, decomposed at about 180 °C. 1-Pyrenylmethyl butanoate was prepared by the same procedure. All of the compounds exhibited only one spot by TLC (Merck silica gel F-254, benzene eluent).

The solvent 2-methyltetrahydrofuran was purified by two vacuum distillations after the preliminary distillation over calcium hydride and dehydration over calcium hydride for 1 week.

Preparation of Sample Solutions. Concentrations of the dilute solutions of a series of bis((1-pyrenylmethoxy)carbonyl)alkanes and 1-pyrenylmethyl butanoate were 1×10^{-5} mol/L and that of the concentrated solution of 1-pyrenylmethyl butanoate was 5.0×10^{-3} mol/L. All of the sample solutions were deaerated by several freeze–thaw cycles at ca. 10^{-5} torr.

Measurements. Absorption spectra were measured by a Shimadzu UV-200S spectrophotometer. For the measurements of fluorescence spectra, a Shimadzu RF-502 spectrofluorophotometer, which gives corrected quantum spectra, was used. The excitation wavelength was 343 nm for all of the samples. Fluorescence quantum yields were determined with reference to that of a solution of quinine sulfate in 1 N sulfuric acid whose reported quantum yield is 0.546[31] where the refractive index of the solutions is corrected. As for the absorbed light intensity (the number of absorbed photons), the absorbance of the sample solution was set to be equal to that of the reference solution. The absorbed light intensity varies with temperature due to the change of the excitation probability, the volume of the sample solution, etc. This effect was corrected by measuring the absorbed light intensity at each temperature. Time-resolved measurements were carried out by single-photon counting (half-width of the light pulse = 2.5 ns) by using the Ortec Inc. system with a Hitachi multichannel analyzer. The temperature of the sample cell in a quartz Dewar was controlled by the flow speed of dry nitrogen, which was precooled by liquid nitrogen, and monitored by a thermocouple.

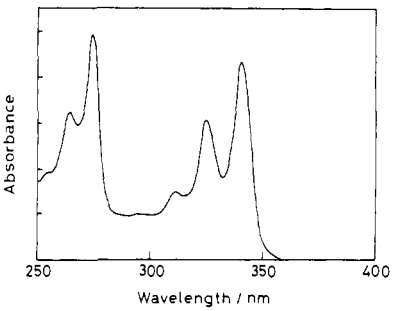

Figure 2. Absorption spectra of PC0, PC1, ..., PC22, and MC4 in MTHF. All the samples have the same spectra.

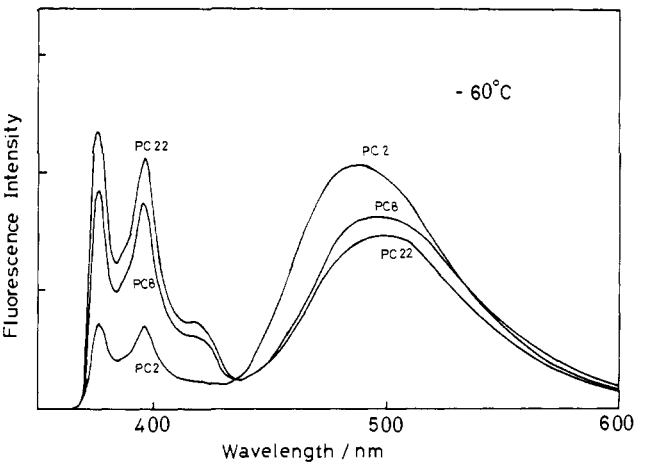

Figure 3. Fluorescence spectra of PC2, PC8, and PC22 at −60 °C.

Results

The absorption spectra of dilute MTHF solutions of the samples PC0, PC1, ..., PC22, and MC4 are shown in Figure 2. The spectra are identical for all of the sample solutions.

(29) (a) Stockmayer, W. H. *Pure Appl. Chem.* **1976**, *15*, 539. (b) Stockmayer, W. H.; Matsuo, K. *Macromolecules* **1972**, *5*, 766. (c) Mashimo, S. *Ibid.* **1976**, *15*, 539.

(30) Ferry, J. D. "Viscoelastic Properties of Polymers", 3rd ed.; Wiley: New York, 1980.

(31) Demas, J. N.; Crosby, G. A. *J. Phys. Chem.* **1971**, *75*, 991.

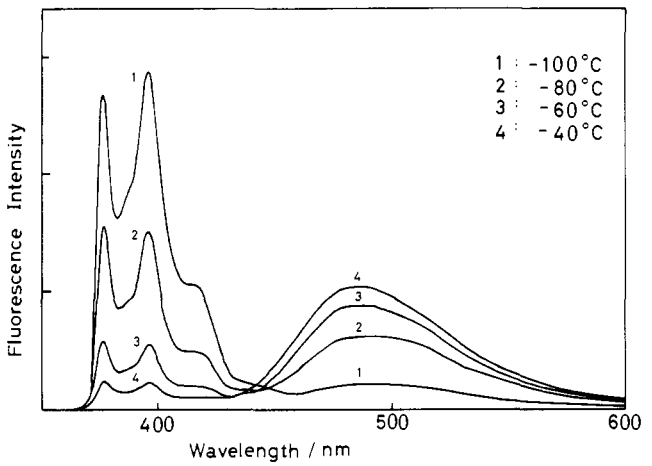

Figure 4. Temperature dependence of fluorescence spectra of PC2: 1, −100 °C; 2, −80 °C; 3, −60 °C; 4, −40 °C.

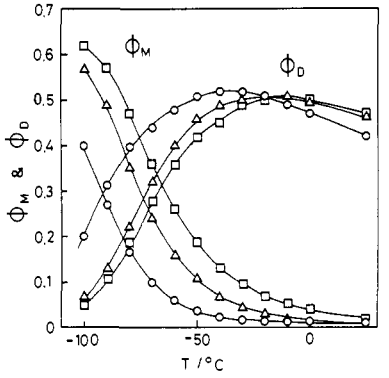

Figure 5. Temperature dependence of Φ_M and Φ_D: (○) PC2; (△) PC8; (□) PC22.

Photostationary State Measurements. The fluorescence spectra of a few samples at −60 °C are shown in Figure 3. The fluorescence spectra of PC1–PC22 (except for PC0[32]) show structureless emission in the wavelength range 450–600 nm besides the quenched monomer fluorescence, while the compound MC4 in such dilute solution presents only the monomer emission. The shapes of the fluorescence spectra of PC1–PC22 are independent of concentration below 10^{-5} mol/L. These facts indicate that the long-wavelength emission of PC1–PC22 is ascribed to the intramolecular excimer that is formed when the excited pyrene moiety on a chain end encounters the other pyrene residue. The observed temperature dependence of the fluorescence spectra for the sample PC2 in the temperature range of −100 to −40 °C is shown in Figure 4. When the temperature was lowered further to −130 °C, the fluorescence spectra of PC1–PC22 showed only the monomer emission and are identical with the fluorescence spectrum of MC4.

Fluorescence quantum yields of the monomer emission Φ_M and the excimer emission Φ_D are summarized in Table I. In separating the total fluorescence quantum yield into Φ_M and Φ_D, we assumed that the shapes of the fluorescence spectra of the monomer emission of PC1–PC22 were identical with that of MC4 at the same temperature. The temperature dependence of Φ_M and Φ_D for a few samples is shown in Figure 5. The monomer emission quantum yield Φ_M decreases monotonously as the temperature increases. The excimer emission quantum yield Φ_D increases as the temperature increases only in the low-temperature range. As the temperature is raised further, Φ_D passes through a maximum

Table I. Fluorescence Quantum Yields and Fluorescence Lifetimes

T, °C	Φ_M	Φ_D	τ_1, ns	τ_2, ns	Φ_M	Φ_D	τ_1, ns	τ_2, ns
	PC1				PC2			
25	0.009	0.42	47	0.5	0.011	0.42	50	1.2
0	0.009	0.47	52	1.0	0.013	0.47	53	2.1
−20	0.010	0.50	58	2.0	0.016	0.51	57	3.5
−40	0.012	0.52	60	4.0	0.025	0.52	59	11
−60	0.032	0.52	63	12	0.062	0.48	65	36
	PC3				PC4			
	0.012	0.42	50	1.4	0.013	0.41	53	1.5
	0.013	0.46	54	3.0	0.014	0.46	55	3.9
	0.020	0.50	57	7.2	0.023	0.51	57	8.0
	0.036	0.51	58	19	0.046	0.51	60	20
	0.093	0.48	68	45	0.10	0.45	67	46
	PC6				PC8			
	0.014	0.46	55	2.1	0.015	0.47	55	2.3
	0.016	0.49	55	4.6	0.019	0.50	56	5.5
	0.027	0.51	58	9.0	0.032	0.51	57	12
	0.058	0.49	58	25	0.070	0.49	61	28
	0.14	0.43	71	52	0.16	0.40	80	54
	PC10				PC14			
	0.019	0.46	55	2.7	0.023	0.46	55	4.0
	0.029	0.49	55	6.0	0.027	0.49	55	9.5
	0.048	0.50	57	14	0.052	0.50	57	21
	0.083	0.46	58	30	0.092	0.46	60	40
	0.18	0.37	86	53	0.19	0.37	93	55
	PC18				PC22			
	0.031	0.48	55	6.7	0.040	0.47	55	8.5
	0.035	0.51	58	13	0.043	0.50	56	22
	0.060	0.51	69	26	0.069	0.50	60	30
	0.12	0.47	84	48	0.13	0.45	72	49
	0.26	0.40	133	55	0.26	0.36	120	55

value at a temperature T_c and begins to decrease. The critical temperature T_c depends on the chain length of the samples. The values of T_c are listed in Table II. As the chain length increases, T_c shifts to higher temperature and finally becomes independent of the chain length for $n \geq 8$ (n denotes the number of methylene units of the sample). The decrease of Φ_D in the high-temperature range is induced by the thermal dissociation of the excimer. The rate of the nonradiative deactivation of the excimer also increases in this temperature range, as can be seen from the fact that Φ_M continues to decrease above T_c. At any given temperature in the low-temperature range, Φ_M increases and Φ_D decreases with increasing chain length. In the high-temperature range, however, the chain-length dependence of Φ_M and Φ_D is not so simple, since the temperature T_c at which Φ_D begins to decrease depends on the chain length.

Wavelengths of the intramolecular excimer emission peak λ_e(max) are listed in Table II. λ_e(max) values of PC1, PC2, PC3, and PC4 are blue shifted compared to the intermolecular excimer emission of MC4 for all of the temperatures. This blue shift becomes smaller as the number of methylene units of the sample increases. For the samples $n \geq 6$, λ_e(max) is identical with that of MC4. The difference of the wavenumbers between the intramolecular and the intermolecular excimer emission peaks is also listed in Table II. This blue shift seems to be caused by the instability of the intramolecular excimer, brought about by the ring strain. This problem will be discussed later.

Time-Resolved Measurements. The transient behavior of the fluorescence emission from both the excimer and the monomer was analyzed by time-resolved measurements. The observed decay curves were simulated by the convolution form integration of the exciting light pulse with an assumed response function of the emission from the monomer and the excimer. As a typical example, the observed decay curve of the monomer emission and the rise and decay curve of the excimer emission for PC18 at 0 °C are shown in Figure 6, where the simulated decay curves are

(32) The sample of PC0 did not show intramolecular excimer emission while the monomer emission was strongly quenched. This fact may indicate that intramolecular end-to-end interaction in PC0 is strong, but the stable fluorescent excimer cannot be formed due to the large strain of the intermediate chain. In the present report, we do not discuss PC0, since the treatment of PC0 is different from other samples and will be reported elsewhere.

Table II. Fluorescence Behavior of Each Sample

	T, °C	PC1	PC2	PC3	PC4	PC6	PC8	PC10	PC14	PC18	PC22
λ_e(max), nm	0	475	481	485	487	490	490	490	490	490	490
	−60	480	486	490	492	495	495	495	495	495	495
$\Delta\nu_e$(max), cm^{-1}	0	644	387	210	126	0	0	0	0	0	0
	−60	631	374	206	123	0	0	0	0	0	0
T_c, °C		−50	−35	−30	−30	−20	←		−15 ~ −10		→

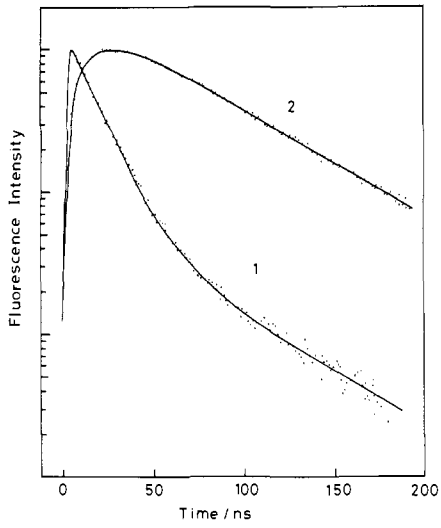

Figure 6. Transient behavior of fluorescence emission from (1) the monomer and (2) the excimer for PC18 at 0 °C: (···) observed decay curves; (—) simulated decay curves with response function of monomer emission $I_M(t) = \exp(-t/58) + 18\exp(-t/13)$ and excimer emission $I_D(t) = \exp(-t/58) - \exp(-t/13)$.

also shown. The monomer emission decays dual-exponentially. The response functions of the monomer emission $I_M(t)$ and the excimer emission $I_D(t)$ were found to be $I_M(t) = \exp(-t/58) + 18\exp(-t/13)$ and $I_D(t) = \exp(-t/58) - \exp(-t/13)$, where time is in nanoseconds. The rise time and the decay time of the excimer emission agree within experimental error (ca. 5%) with the decay time of the fast component and that of the slow one of the monomer emission, respectively. In any case, we can precisely determine the rise time τ_2 and the decay time τ_1 of the excimer emission. On the other hand, it is very difficult to determine the decay times of the monomer emission when the fraction of the fast decay or the slow one is very small or the decay time of the fast component is not so different from that of the slow one. Even in such a case, we can simulate the decay curve of the monomer emission well by τ_1 and τ_2 obtained from the excimer emission, using the fraction of the fast decay component as an adjustable parameter. This means that the response functions of the monomer emission $I_M(t)$ and the excimer emission $I_D(t)$ are expressed by eq 1 and eq 2, respectively, for all of the samples and in the whole temperature range, where C_M and C_D are constants. The values τ_1 and τ_2 determined from the excimer emission for each sample at various temperatures are summarized in Table I. It should be noted that the weighting factor of the fast decay component of the monomer emission A in eq 1 is very large at 25 °C and, after slight increase, decreases with decreasing temperature. Finally, A reaches to zero below ca. −80 °C for the samples $n \geq 3$ and below ca. −100 °C for the samples $n \leq 2$.

$$I_M(t) = C_M[\exp(-t/\tau_1) + A\exp(-t/\tau_2)] \quad (1)$$

$$I_D(t) = C_D[\exp(-t/\tau_1) - \exp(-t/\tau_2)] \quad (2)$$

In general, the deviation from the single exponential of the monomer emission suggests that either the excimer dissociation occurs or multiple modes of chain motion take part in the intramolecular excimer formation. As mentioned above, τ_1 and τ_2 estimated from the excimer emission agree with those estimated from the monomer decay, and no other decay or rise components were found in either the monomer emission or the excimer emission. This indicates that the deviation from the single exponential of the monomer emission is due to the excimer dissociation and the intramolecular end-to-end excimer formation is dominated by a single mode of chain motion. The table shows that both τ_1 and τ_2 become monotonously longer as the temperature decreases. In the limit of low temperatures, τ_1 and τ_2 approach asymptotically to 250 and 55 ns, respectively. At a certain temperature, τ_1 and τ_2 decrease as the chain length decreases.

Scheme I

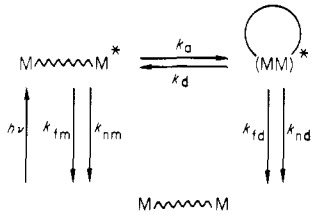

Discussion

Kinetics of Intramolecular End-to-End Excimer Formation. In order to describe intramolecular end-to-end excimer formation, we adopted the reaction given in Scheme I, which was first introduced by Förster[33] and confirmed for various intermolecular excimer systems.[34] Here, k_{fm} and k_{fd}, k_{nm} and k_{nd}, and k_a and k_d are the rate constants for the fluorescence from the monomer and the excimer, for the nonradiative processes from the monomer and the excimer, and for the intramolecular excimer formation and the dissociation process, respectively. Kinetic equations according to the above scheme lead to the following expressions. For the photostationary state, the quantum yields of the monomer fluorescence Φ_M and of the excimer fluorescence Φ_D, respectively, are

$$\Phi_M = k_{fm}Y/(XY - k_ak_d) \quad (3)$$

$$\Phi_D = k_{fd}k_a/(XY - k_ak_d) \quad (4)$$

where

$$X = k_{fm} + k_{nm} + k_a \quad (5)$$

$$Y = k_{fd} + k_{nd} + k_d \quad (6)$$

For excitation by a δ-function light pulse at $t = 0$, the fluorescence response functions of the monomer $I_M(t)$ and of the excimer $I_D(t)$, respectively, are

$$I_M(t) = k_{fm}(\lambda_2 - X)(\exp(-\lambda_1 t) + A\exp(-\lambda_2 t))/(\lambda_2 - \lambda_1) \quad (7)$$

$$I_D(t) = k_ak_{fd}(\exp(-\lambda_1 t) - \exp(-\lambda_2 t))/(\lambda_2 - \lambda_1) \quad (8)$$

where

$$\lambda_{1,2} = [X + Y \mp ((Y - X)^2 + 4k_ak_d)^{1/2}]/2 \quad (9)$$

$$A = (X - \lambda_1)/(\lambda_2 - X) \quad (10)$$

$$X + Y = \lambda_1 + \lambda_2 \quad (11)$$

$$XY = \lambda_1\lambda_2 + k_ak_d \quad (12)$$

Fluorescence response functions of the monomer and the excimer obtained according to the kinetic scheme (eq 7 and eq 8) correspond to the observed fluorescence response functions of the

(33) Förster, Th.; Seidel, H. P. *Z. Phys. Chem. (Wiesbaden)* **1965**, *45*, 58.
(34) Birks, J. B. "Photophysics of Aromatic Molecules"; Wiley-Interscience: New York, 1970, Chapter 7.

Table III. Rate Constants k_a, k_d, k_{fd}, k_{nd} ($\times 10^{-7}/s^{-1}$)

T, °C	PC1	PC2	PC3	PC4	PC6	PC8	PC10	PC14	PC18	PC22
(a) Rate Constants k_a for Intramolecular End-to-End Excimer Formation Process										
25	184	77	65	61	44	40	32	22	13	9.3
0	93	44	31	24	20	17	14	9.6	6.9	4.3
−20	47	26	13	12	10	7.6	5.8	4.1	3.4	2.9
−40	24	8.6	5.1	4.5	3.5	2.9	2.5	2.0	1.5	1.4
−60	7.6	2.7	1.9	1.8	1.2	1.0	0.85	0.81	0.55	0.46
(b) Rate Constants k_d for Intramolecular End-to-End Excimer Dissociation Process										
25	15.0	6.2	5.7	5.4	3.6	3.4	3.8	2.7	1.8	1.8
0	5.9	3.3	1.7	1.1	0.98	0.93				
−20	2.1	1.8								
(c) Rate Constants k_{fd} for Fluorescence Process of Intramolecular End-to-End Excimer										
25	0.97	0.91	0.92	0.85	0.92	0.95	0.95	0.97	1.0	1.1
0	0.97	0.96	0.91	0.89	0.95	0.97	1.1	0.98	0.98	0.93
−20	0.91	0.97	0.94	0.97	0.97	0.99	1.1	1.0	0.84	0.97
−40	0.90	0.93	0.91	0.94	0.96	0.97	1.1	0.95	0.77	0.94
−60	0.91	0.76	0.82	0.82	0.96	0.91	0.95	0.90	0.99	1.2
(d) Rate Constants k_{nd} for Nonradiative Process of Intramolecular End-to-End Excimer										
25	1.3	1.2	1.2	1.2	1.0	1.0	1.0	1.0	1.0	1.1
0	1.1	1.0	1.0	1.0	0.94	0.90	0.98	0.92	0.82	0.65
−20	0.88	0.88	0.87	0.85	0.84	0.83	0.90	0.82	0.63	0.73
−40	0.80	0.78	0.58	0.75	0.80	0.76	0.89	0.77	0.51	0.66
−60	0.73	0.45	0.56	0.66	0.71	0.70	0.78	0.69	0.31	0.55

monomer and the excimer (eq 1 and eq 2), where $\tau_1 = \lambda_1^{-1}$ and $\tau_2 = \lambda_2^{-1}$. Equations 3 and 4 with eq 12 yield

$$\Phi_M = k_{fm}Y/\lambda_1\lambda_2 = k_{fm}Y\tau_1\tau_2 \quad (3')$$

$$\Phi_D = k_{fd}k_a/\lambda_1\lambda_2 = k_{fd}k_a\tau_1\tau_2 \quad (4')$$

The values τ_1 and τ_2 in eq 3′ and 4′ can be measured. Then, when the rate constants for the fluorescence and the nonradiative process of the monomer, k_{fm} and k_{nm}, are given, all of the rate constants in the scheme can be determined by eq 3′, 4′, 11, and 12. In this study the values k_{fm} and k_{nm} are assumed to be those of the model compound MC4, which were determined by measuring the fluorescence quantum yield and its lifetime in an extremely dilute MTHF solution. The values of k_{fm} and k_{nm} were 0.22×10^7 and 0.18×10^7 s^{-1}, respectively, and almost independent of temperature in the range of our investigation. In this report, therefore, these values were used irrespective of temperature. The values k_a and k_d were calculated as described above by the equations $k_a = X - k_{fm} - k_{nm}$ or $k_d = (XY - \lambda_1\lambda_2)/k_a$. The obtained values of k_a, k_d, k_{fd}, and k_{nd} are summarized in Table III.

Frequency of Intramolecular End-to-End Collisions. The rate constant for the intramolecular end-to-end excimer formation process k_a corresponds to the frequency of collisions between an excited pyrene moiety and another pyrene residue on a chain within its lifetime, since the excimer formation process is diffusion controlled. As for the intramolecular end-to-end collisional frequency on a chain, the following factors must be considered. (i) The initial conformational distribution of the compounds immediately after the excitation of the pyrene group by light is in thermal equilibrium. (ii) From this initial state, the conformation of a chain with an excited pyrene moiety on one end changes by thermal motion so that the distance between two end pyrene groups fluctuates and they meet to form an end-to-end excimer. The rate of the conformational transition is an important factor in determining the end-to-end collisional frequency of a chain. The conformational transition rate is quantitatively expressed as a relaxation time of the molecular motion. Hence, it is a significant problem to verify which modes take part in the end-to-end collisions. (iii) For an end-to-end excimer to form, two end pyrene residues must encounter each other within the lifetime of an excited pyrene residue. If the rate of the conformational transition of a chain is much faster than the self-deactivation rate of the excited pyrene residue, the excited pyrene residue is able to encounter another pyrene residue on a chain. However, if the conformational transition rate is slower than the deactivation rate of the excited pyrene residue, only those polymer chains with conformations in which two pyrene groups are in close vicinity to each other at the instant of excitation can form the intramolecular excimer. The situations covered in this study are believed to lie between these limiting cases.

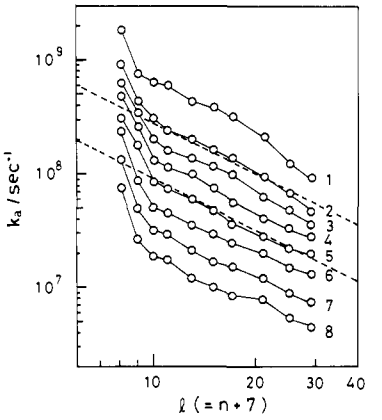

Figure 7. Chain-length dependence of k_a at various temperatures. Slopes of dashed lines are −1.5: 1, 25 °C; 2, 0 °C; 3, −10 °C; 4, −20 °C; 5, −30 °C; 6, −40 °C; 7, −50 °C; 8, −60 °C.

In Figure 7, k_a is plotted as a function of the chain length l, the number of bonds between two end pyrene residues ($l = n + 7$), at various temperatures. The rate constant k_a is approximately proportional to the −1.5 power of the chain length l, except for PC1 and PC2. A similar result was obtained for the intramolecular end-to-end electron-exchange system, $N(CH_2)_nN^{-}\cdot$ (N = naphthyl group), which was determined by the analysis of line shapes in ESR spectra.[10,35] The result that the intramolecular end-to-end collisional frequency is proportional to $l^{-1.5}$ contrasts with the chain-length dependence of the ring-closure probability evaluated by covalent ring closure.[2,3,36,37] It is well-known that the ring-closure probability has a peak at the chain length about $l = 15$. This indicates that the intramolecular end-to-end collisional frequency is independent of the ring-closure probability.

(35) Recently, reinterpretation of Shimada and Szwarc's results was presented by Winnik (*J. Am. Chem. Soc.* **1981**, *103*, 708). It was stated that the electron exchange is not diffusion controlled, so the results should be interpreted in terms of conformationally controlled cyclization. Excimer formation of pyrene was confirmed to be diffusion controlled and the critical distance is 3.5–4.0 Å (see ref 34 in this paper). Present results should be interpreted in terms of a diffusion-controlled process.

(36) Flory, P. J. "Statistical Mechanics of Chain Molecules"; Interscience: New York, 1969; Chapter 8.

(37) Sisido, M. *Macromolecules* **1971**, *4*, 737.

Table IV. Activation Energies E_a and Frequency Factors A_a for Intramolecular End-to-End Excimer Formation

	PC1	PC2	PC3	PC4	PC6	PC8	PC10	PC14	PC18	PC22
E_a/kcal mol^{-1}	4.8	5.2	5.2	5.1	5.3	5.3	5.2	5.1	4.8	4.8
$A_a \times 10^{-12}$/s^{-1}	6.2	6.8	4.2	3.0	3.5	2.9	1.9	1.1	0.47	0.39

The ring-closure probability is governed by the distribution of the conformations in equilibrium. On the other hand, the collisional frequency is determined both by the conformational distribution and by the rate of the conformational change.

Zachariasse et al.[12] have studied the intramolecular end-to-end excimer of α,ω-bis(1-pyrenyl)alkanes at 22 °C and determined the intensity ratio of the excimer and monomer emission, Φ_D/Φ_M. It was found that the ratio has a second peak at 1,13-bis(1-pyrenyl)tridecane. According to the reaction kinetics, the ratio Φ_D/Φ_M is represented by

$$\frac{\Phi_D}{\Phi_M} = \frac{k_{fd}k_a}{k_{fm}(k_{fd} + k_{nd} + k_d)}$$

For the present system, k_{fm} and k_{fd} are independent of chain length while k_d and k_{nd} decrease with increasing chain length, especially for PC1, PC2, PC3, and PC4 (see Table III). The decrease of k_d and k_{nd} may disappear in sufficiently long chains.[16a,b] So long as k_d and k_{nd} depend on chain length, the chain-length dependence of the ratio Φ_D/Φ_M does not correspond to that of the excimer formation rate k_a. For evaluation of the intramolecular end-to-end collisional frequency as a function of the chain length, time-resolved analysis is necessary in addition to photostationary measurements.

Theoretical treatment of an intramolecular end-to-end diffusion-controlled reaction was first undertaken by Wilemski and Fixman[38] (WF) on the basis of a generalized diffusion equation of a polymer chain. They solved the equation for the Rouse chain by using the closure approximation. Their results show that the intramolecular reaction rate is determined only by the longest relaxation time of the Rouse chain. Perico and Cuniberti[14b] examined the end-to-end diffusion-controlled reaction in the case of partial draining, following the WF theory, and showed that the intramolecular reaction rate constant in the case of partial draining has relevant contribution from all of the modes of the bead-spring chain. In application of their conclusions to our experimental results, the following points must be considered.

First, the chain length of our samples is so short that it is not clear whether the statistical-chain models, for example, the bead-spring model or the harmonic-spring model, are valid or not. Second, the pyrene residue is so bulky compared to the chain length that the motion of the chain may be affected by the residue, while their theories are concerned with chains without end groups. Third, experimentally it is difficult to observe modes of motion with longer relaxation times than the lifetime of the excited pyrene residue, which is deactivated not only by the intramolecular end-to-end excimer formation but also by the self-deactivation process of the residue. As mentioned before, our decay analysis shows that the intramolecular end-to-end collision is dominated by only one relaxation time. Therefore, in spite of above-mentioned factors, it seems still valid to adopt the WF conclusion that the intramolecular reaction rate is determined only by the longest relaxation time of a chain, so long as the intramolecular end-to-end excimer formation rate is sufficiently fast for the self-deactivation process to be negligible.

The intramolecular end-to-end excimer formation rate k_a is of the order of 10^9–10^7 s^{-1} above −60 °C, which is much faster than the self-deactivation rate (4.0×10^6 s^{-1}). This indicates that an excited pyrene residue on one end is mostly able to encounter the pyrene residue at the other end of the chain within its lifetime, regardless of the initial conformation of the chain. In such a temperature region, k_a must be determined by the longest relaxation time of a polymer chain, according to Wilemski and Fixman. Therefore, the results may represent the chain-length dependence of the longest relaxation time of our samples.

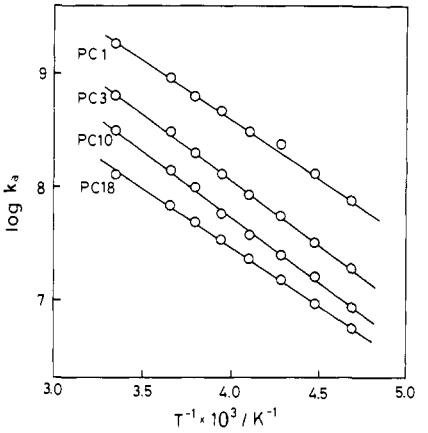

Figure 8. Temperature dependence of k_a for the samples PC1, PC3, PC10, and PC18.

Temperature Dependence of k_a. Arrhenius plots of k_a for several samples above −60 °C are shown in Figure 8. Apparent activation energies E_a and the frequency factors A_a derived from these plots are listed in Table IV. The results agree with the previous results obtained from the photostationary state measurements.[13] E_a seems to show a maximum value at about PC6 or PC8 but may be constant (ca. 5.0 kcal/mol), taking into account the experimental errors. On the other hand, it was previously reported that E_a depends on the molecular structure of the chains.[39] The activation energy E_a represents the energy-barrier height for the intramolecular end-to-end excimer formation and will present significant information on conformational transitions of the chain.

It is predicted[40] that temperature dependence of the conformational transition rates or relaxation times of molecular motions of a polymer chain, in which the internal rotation potential is ignored, is identical with that of the frictional coefficient in the surrounding medium whose temperature dependence roughly corresponds to that of solvent viscosity η. The activation energy E_η of the viscosity of the solvent MTHF is 1.8 kcal/mol,[41] which is relatively small compared with E_a. This suggests that the internal rotation potential in the conformational transition of a polymer chain must be considered. The conformational transition across the internal rotation barrier has been discussed by Helfand[42] and Iwata,[43] where Kramers' theory[44] was applied to the transition between rotational isomeric states of a local chain in viscous media. They obtained the probability P per unit time that a local chain located initially in a well escapes along the transient path, crossing a potential-energy barrier $\Delta E^\ddagger$ where I and ζ are the moment of

$$P = \frac{\gamma_A^{1/2}}{2\pi I \gamma_B^{1/2}}\left[\left(\frac{1}{4}\zeta^2 + I\gamma_B\right)^{1/2} - \frac{1}{2}\zeta\right] \exp(-\Delta E^\ddagger/RT) \quad (13)$$

inertia and the rotational friction coefficient of the local chain, respectively, and γ_A and γ_B are the force constants of the potential well and the potential barrier, respectively. In the theory, it was assumed that $\Delta E^\ddagger$ is larger than $5RT$ and that a Maxwell distribution in the potential well is maintained. This theory is concerned with local conformational changes of a chain. On the other hand, for the intramolecular end-to-end excimer formation,

(38) Wilemski, G.; Fixman, M. *J. Chem. Phys.* **1974**, *60*, 866, 878.

(39) Kanaya, T.; Yamamoto, M.; Nishijima, Y. *Rep. Prog. Polym. Phys. Jpn.* **1980**, *23*, 547.

(40) Yamakawa, H. "Modern Theory of Polymer Solutions"; Harper and Row: New York, 1971.

(41) Szwarc, M. "Carbanion, Living Polymers, and Electron-Transfer Processes"; Interscience: New York, 1968, Chapter 5.

(42) Helfand, E. *J. Chem. Phys.* **1971**, *54*, 4651.

(43) Iwata, K. *J. Chem. Phys.* **1973**, *58*, 4184.

(44) Kramers, H. A. *Physica (Amsterdam)* **1940**, *7*, 284.

conformational change of a whole chain must be considered. The conformational change of a whole chain is, however, represented by the succession of local conformational changes and the local conformational change is the rate-determining step of the conformational transition. This picture is supported by the finding that E_a is independent of chain length.

The apparent activation energy E_c for the conformational transition obtained from eq 13 in the case of large friction, $\zeta^2 \gg 4I\gamma_B$, is

$$E_c = E_\eta + \Delta E^\ddagger \tag{14}$$

and in the case of small friction, $\zeta^2 \ll 4I\gamma_B$, is

$$E_c = \Delta E^\ddagger \tag{15}$$

For a description of end-to-end collision, it is convenient to employ the rate constant for the mutual diffusion $k_{m,d}$ between two ends. The explicit form of $k_{m,d}$ is not known, while the temperature dependence of $k_{m,d}$ may be the same as that of the probability P, since the mutual diffusion is governed by the succession of local conformation changes.

According to the Einstein–Smoluchowski diffusion theory,[34] the intermolecular collisional rate k_{diff} is proportional to (T/η), so that the activation energy for this process E_{diff} can be obtained by plotting log (T/η) vs. $1/T$. When intermolecular excimer formation is governed only by the collisional process, the activation energy for the intermolecular excimer formation $E_{a,inter}$ should be identical with E_{diff}. The value of E_{diff} was obtained as 2.3 kcal/mol for MTHF, and it was found that $E_{a,inter}$ of pyrene or MC4 in MTHF is 3.6 kcal/mol, 1.3 kcal/mol higher than E_{diff}. This is because either (a) the reaction probability per collision depends on temperature or (b) there exists a certain chemical process after the collision. The physical meanings of the two concepts are very different,[45] and at present there is no way to choose between them. Inter- and intramolecular excimer formation will now be considered on the basis of both of these concepts.

In case a, the intermolecular excimer formation rate $k_{a,inter}$ is represented by

$$k_{a,inter} = k_{diff}p \tag{16}$$

where p is reaction probability per collision. Under the assumption of the Arrhenius form of p with activation energy E_p, the activation energy for the intermolecular excimer formation $E_{a,inter}$ is of the form

$$E_{a,inter} = E_{diff} + E_p \tag{17}$$

E_p was obtained to be 1.3 kcal/mol, since $E_{a,inter}$ for the excimer formation of pyrene or MC4 in MTHF is 3.6 kcal/mol and E_{diff} is 2.3 kcal/mol. If the reaction probability per collision for the intramolecular excimer formation has the same temperature dependence as in the intermolecular case, the apparent activation energy for the intramolecular excimer formation E_a is represented by

$$E_a = E_c + E_p \tag{18}$$

since k_a is of the form

$$k_a = k_{m,d}p \tag{19}$$

The viscosity of the solvent MTHF is very small ($\eta = 1.50 \times 10^{-2}$ P at −60 °C[41]) so that the apparent activation energy for the conformational transition E_c is given by eq 15. Then, the potential energy barrier height of the chain $\Delta E^\ddagger$ is estimated to be 3.7 kcal/mol for $E_a = 5.0$ and $E_p = 1.3$ kcal/mol.

In case b, the intermolecular excimer rate constant $k_{a,inter}$ is given by[46,47]

$$k_{a,inter}^{-1} = k_{diff}^{-1} + k_r^{-1} \tag{20}$$

where k_r is the rate constant for the reaction process after the collision, which has the Arrhenius form with activation energy E_r. The activation energy $E_{a,inter}$ is of the form

$$E_{a,inter} = \frac{E_{diff}}{1 + (k_{diff}/k_r)} + \frac{E_r}{1 + (k_r/k_{diff})} \tag{21}$$

By using the observed $E_{a,inter}$ value (3.6 kcal/mol) and E_{diff} value (2.3 kcal/mol), E_r can be calculated from eq 21 when the ratio of the frequency factor of k_r to that of k_{diff}, i.e., A_r/A_{diff}, is given. In the case of A_r/A_{diff} being less than 1.0, E_r is 3.6 kcal/mol. Even when A_r/A_{diff} is 10.0, E_r does not exceed 3.8 kcal/mol. This means that the temperature dependence of $k_{a,inter}$ is governed mostly by that of the chemical process. The temperature dependence of the intramolecular excimer process can be treated in the same manner as for the intermolecular case, by using the rate constant of the mutual diffusion between two ends of the chain $k_{m,d}$. The rate constant for the intramolecular excimer formation k_a and its activation energy E_a are expressed by

$$k_a^{-1} = k_{m,d}^{-1} + k_r^{-1} \tag{22}$$

$$E_a = \frac{E_c}{1 + (k_{m,d}/k_r)} + \frac{E_r}{1 + (k_r/k_{m,d})} \tag{23}$$

Assuming the E_r value estimated above to be 3.6 kcal/mol and E_a to be 5.0 kcal/mol, then E_c is calculated to be 5.0 kcal/mol if $A_{m,d}/A_r < 1$. Even when $A_{m,d}/A_r = 10$, E_c is 5.2 kcal/mol. This result of E_c means that the activation energy of the intramolecular excimer E_a is determined mostly by that of the conformational transition process E_c. The energy-barrier height for the internal rotation of the chain $\Delta E^\ddagger$ is estimated from eq 15 to be 5.0 kcal/mol.

The values of the energy-barrier height $\Delta E^\ddagger$ estimated by the two treatments (a and b) are 3.7 and 5.0 kcal/mol, respectively, and both of them satisfy the assumption of Kramers' theory, $\Delta E^\ddagger \geq 5RT$. At the present stage, we cannot conclude which treatment is appropriate for the intramolecular excimer formation, and further theoretical and experimental work is necessary.

Strain of a Cyclized Chain. As discussed in the previous section, rate studies of the intramolecular end-to-end excimer formation have provided information on the end-to-end collisional frequency of a chain. On the other hand, emission properties of the intramolecular end-to-end excimer present information on the strain of a chain that is closed to form a ring. The intramolecular excimer, which is produced after passing through the energy barrier, is stabilized by an electronic interaction (the so-called excimer interaction) between two pyrene residues on a chain. The cyclic state may, however, be in a higher energy state due to the strain of the chain. Therefore, the nature of the excimer emission is affected by the strain of a cyclized chain.

As for the nature of the intramolecular excimer, the peak wavelength of the excimer emission, $\lambda_e(max)$, and the excimer rate constants, k_d, k_{fd}, and k_{nd}, were obtained as described in the previous section.

The wavelengths of the excimer emission peaks $\lambda_e(max)$ are blue shifted for PC1, PC2, PC3, and PC4, compared to that of the intermolecular excimer emission peak of MC4 (see Table II). The energy difference between the excimer state and the ground state corresponds to $h\nu_e(max)$, where h is Planck's constant and $\nu_e(max)$ is the wavenumber of the excimer emission peak. Since the energy level of PC1–PC22 and MC4 in the ground state should be identical, the excimer states are considered to be in a higher energy state than the intermolecular excimer of MC4. The increment of energy of the intramolecular excimer of PC1–PC4 may be brought about by the strain of the cyclized chains and this magnitude corresponds to $h\Delta\nu_e(max)$. The strain is largest in PC1 and decreases with increasing chain length. For $n \geq 6$, $\lambda_e(max)$ is no longer affected by the strain of the cyclized chain; i.e., the

(45) In the former concept, the reaction probability per collision is considered to be a part of the collisional process so that the excimer formation rate is expressed by the collisional rate times the probability. The latter concept predicts that the excimer formation is a stepwise process so that the total reaction rate is represented by a harmonic mean of the rate constants for each step.

(46) Marcus, R. A. *Faraday Discuss. Chem. Soc.* **1960**, *29*, 129.
(47) Noyes, R. M. *Prog. React. Kinet.* **1961**, *1*, 129.

strain is negligible. Because of the strain, the conformation of the intramolecular excimers of PC1, PC2, PC3, and PC4 may deviate from the sandwich geometry, which is the most stable conformation of an excimer.[34]

Coops et al.[48] have measured the excess combustion enthalpies for various cycloalkanes. They found that 8-, 9-, 10-, and 11-membered rings have rather high strain energy, while larger cycloalkanes and cycloheptane have less strain, and cyclohexane has zero strain energy. The number of chain atoms of our samples, PC1, PC2, PC3, and PC4, is 7, 8, 9, and 10, respectively. The emission behavior of the strained excimer of our samples corresponds to the results of Coops et al., though the chains of our samples contain heteroatoms.

The dissociation rate of the excimer (k_d, Table IIIb) depends on chain length. At a given temperature, k_d becomes larger as the chain length decreases, which is clearly observed for PC1, PC2, PC3, and PC4. As mentioned above, PC1, PC2, PC3, and PC4 have a rather high strain of the chain when they are cyclized. The chain-length dependence of k_d shows that these excimers can easily dissociate because of the rather high strain of the cyclized chain. For the samples with $n \geq 6$, k_d gradually decreases with increasing chain length, while $\Delta\nu_e(\max) = 0$. It seems that k_d is more sensitive to the strain of the cyclized chain than $\Delta\nu_e(\max)$. It should be noted that k_d is independent of chain length for sufficiently long chains[16b] where cyclization does not induce strain energy.

The rate constant for the nonradiative process from the excimer (k_{nd}, Table IIId) decreases as the chain length increases. This is also due to the instability of the excimer, which is brought about by the strain of the cyclized chain. However, the rate constant for the fluorescence from the excimer (k_{fd}, Table IIIc) is identical for all samples. This may indicate that the emission process, whose rate is determined by the transition moment,[49] is less sensitive to the instability of the excimer than the nonradiative process.

Concluding Remarks

In the present work, it has been shown that the study of the intramolecular end-to-end excimer gives useful information on both dynamic behavior of the chain and the strain of the cyclized chain. As for the dynamic behavior, the intramolecular end-to-end collisional frequency was obtained as a function of the chain length and the temperature. The frequency, which corresponds to k_a, was proportional to the −1.5 power of the chain length in the temperature range above −60 °C. The temperature dependence of k_a gave an apparent activation energy of ca. 5 kcal/mol for the intramolecular end-to-end excimer formation for all of the samples. This activation energy was analyzed in terms of Kramers' theory to evaluate the energy-barrier height for the conformational transition. The strain of the cyclized chain was evaluated by the emission properties of the intramolecular excimer. The wavelengths of the excimer emission peaks were blue shifted by about 15, 9, 5, and 3 nm for PC1, PC2, PC3, and PC4, respectively, at −60 °C, since these compounds are highly strained in the cyclized state.

In the next paper, the ring-closure probability of the chain, which is governed by the conformational distribution in thermal equilibrium, will be discussed on the basis of intramolecular end-to-end excimer formation.

Registry No. PC0, 81496-96-0; PC1, 67512-97-4; PC2, 67512-98-5; PC3, 67512-99-6; PC4, 67513-00-2; PC6, 67513-01-3; PC8, 67513-02-4; PC10, 67513-03-5; PC14, 67513-04-6; PC18, 67513-05-7; PC22, 67513-06-8; MC4, 81478-03-7.

(48) Coops, J.; Kamp, H. van; Lambregests, W. A.; Wisser, J.; Decker, H. *Recl. Trav. Chim. Pays-Bas* **1960**, *79*, 1226.

(49) Mataga, N.; Kubota, T. "Molecular Interactions and Electronic Spectra"; Marcel Dekker: New York, 1970, Chapter 3.

Fragmentation of Metastable CH_4^+ Ions and Isotopic Analogues. Kinetic Energy Release Distributions and Tunneling through a Rotational Barrier: Experiment and Theory

A. J. Illies, M. F. Jarrold, and M. T. Bowers*

Contribution from the Department of Chemistry, University of California, Santa Barbara, California 93106. *Received October 13, 1981*

Abstract: The fragmentation of metastable CH_4^+, CD_3H^+, and CD_4^+ ions has been studied with use of mass analyzed ion kinetic energy spectrometry (MIKES). Kinetic energy release distributions were derived from the MIKES peaks. The average kinetic energy release and metastable intensity were found to increase with ion source temperature. Appearance potential measurements indicated that the metastable reaction arises from CH_4^+ ions with internal energy close to the thermochemical threshold for fragmentation to give ground state $CH_3^+(^1A_1) + H(^2S)$. The experimental data suggest that the origin of the metastable process is tunneling through a centrifugal barrier. A statistical model is presented and predictions of the model are compared with the experimental data.

The fragmentation of metastable CH_4^+ ions and its isotopic analogues via reaction 1 has been the subject of a number of

$$CH_4^+ \rightarrow CH_3^+ + H \quad (1)$$

studies.[1-6] The principal reason for this interest is that the observation of a metastable with a mass spectrometer requires a lifetime in the range 10^{-6}–10^{-3} s, but statistical theories predict a lifetime in the nanosecond range for CH_4^+. Hills et al.[1] attempted to reconcile the observation of the metastable by mod-

(1) L. P. Hills, M. L. Vestal, and J. H. Futrell, *J. Chem. Phys.*, **54**, 3834 (1971).
(2) C. E. Klots, *J. Phys. Chem.*, **75**, 1526 (1971).
(3) C. E. Klots, *Chem. Phys. Lett.*, **10** 422 (1971).
(4) B. H. Solka, J. H. Beynon, and R. G. Cooks, *J. Phys. Chem.*, **79** 859 (1975).
(5) V. H. Dibeler and H. M. Rosenstock, *J. Chem. Phys.*, **39**, 1326 (1963).
(6) J. P. Flamme, J. Momigny, and H. Wankenne, *J. Am. Chem. Soc.*, **98**, 1045 (1976).

0002-7863/82/1504-3587$01.25/0